PBR ELECTRONICS, INC.
P. O. BOX 752
ATHENS, ALABAMA 35611

(NASA-CR-120741) RAMAN BACKSCATTER MEASUREMENT RESEARCH ON WATER VAPOR SYSTEMS Final Report (PBR Electronics, Inc.) 37 p HC $3.75 CSCL 04A

N75-22977

Unclas
G3/46 20360

RAMAN BACKSCATTER MEASUREMENT RESEARCH ON WATER VAPOR SYSTEMS

FINAL REPORT

PREPARED FOR

GEORGE C. MARSHALL SPACE FLIGHT CENTER

MARSHALL SPACE FLIGHT CENTER, ALABAMA 35812

NASA CONTRACT NAS8-30805

PRINCIPAL INVESTIGATOR: DR. GARY L. WORKMAN

10 APRIL 1975

PBR ELECTRONICS, INC.
P. O. BOX 752
ATHENS, ALABAMA 35611

RAMAN BACKSCATTER MEASUREMENT RESEARCH ON WATER VAPOR SYSTEMS

FINAL REPORT

PREPARED FOR

GEORGE C. MARSHALL SPACE FLIGHT CENTER

MARSHALL SPACE FLIGHT CENTER, ALABAMA 35812

NASA CONTRACT NAS8-30805

PRINCIPAL INVESTIGATOR: DR. GARY L. WORKMAN

10 APRIL 1975

ABSTRACT

Raman backscatter techniques have proven to be a useful remote sensing tool, whose full potential has not been realized at this time. The type of information available from laser probes in atmospheric studies are reviewed here and detection levels for known Raman cross-sections are calculated using the laser radar equation. Laboratory experiments performed for H_2O, N_2, SO_2, 02 and HCl indicate that accurate wavelength cross-sections need to be obtained, as well as more emphasis on obtaining accurate Raman cross-sections of molecular species at wavelengths in the ultraviolet.

TABLE OF CONTENTS

		PAGE
A.	INTRODUCTION	1
B.	THE RAMAN BACKSCATTER TECHNIQUE	2
C.	INSTRUMENTATION	7
D.	CROSS-SECTIONS OF MOLECULAR SPECIES	16
E.	EXPERIMENTAL DETAILS	19
F.	APPLICATION TO ATMOSPHERIC PROCESSES	25
G.	RECOMMENDATIONS FOR FURTHER LABORATORY RESEARCH	30
H.	BIBLIOGRAPHY	32

A. INTRODUCTION

A number of investigators [1-5] have probed the atmosphere with laser excitation and monitored specific molecular constituents by measuring the Raman emission from these molecules. A number of these investigations have been concerned with meteorological observations, as well as potential applications to monitoring pollutants in the atmosphere. [4, 6] Since the Raman cross-sections for particular molecules are important in that they determine the sensitivity of the technique, a comprehensive review of experimental determinations is given here.

Another objective of this program has been to review the literature and analyze critically the data from lidar systems to date. In order to perform this task adequately, we have made experimental measurements on various atmospheric species such as N_2, O_2, and H_2O. Also, we have computed signal intensities for several molecular species at various distances from a given laser source and of predetermined energy. Included within this report is also a series of spectral plots of Stokes bands of some known molecular species for several popular laser lines.

The full capability of the laser Raman backscattering technique still has not been realized. With the ever improving technological developments in laser systems, as well as signal handling techniques, the future of remote sytems is optimistic indeed. When one also considers the various possible approaches such as land based, airplane or satellite systems, the amount of information on molecular constitutents will be extensive indeed.

B. THE RAMAN BACKSCATTER TECHNIQUE

The Raman effect is one member of a wide class of light scattering processes caused by molecular interactions with light. The most significant advantage of Raman scattering compared to most of the others is that the scattered radiation occurs at a wavelength shifted away from the exciting wavelength. This wavelength shift is characteristic of the molecular species being excited and thus provides a convenient, but relatively insensitive technique for molecular identification or molecular density measurements. A schematic illustrating the relationship of energy levels of a molecular species for Raman and fluorescent processes is given in Figure 1. Since the Raman effect does not require excitation to a molecular energy level or bound state, the process occurs in about 10^{-12} seconds or less. Normally fluorescent emission occurs in 10^{-7} to 10^{-9} seconds, but this type of emission is much more intense. A comparison of the types of processes considered for atmospheric probes and some appropriate comments are given in Table I.

TABLE I

Scattering Process	Characteristic Feature	Cross Section (cm^2/ster)
Mie	Most prominant for particles	10^{-27} to 10^{-8}
Rayleigh	Particles and molecules	10^{-27}
Raman	Molecular	10^{-29} to 10^{-30}
Resonance Raman	Molecular	10^{-23}
Fluorescence	Molecular	10^{-16} or less

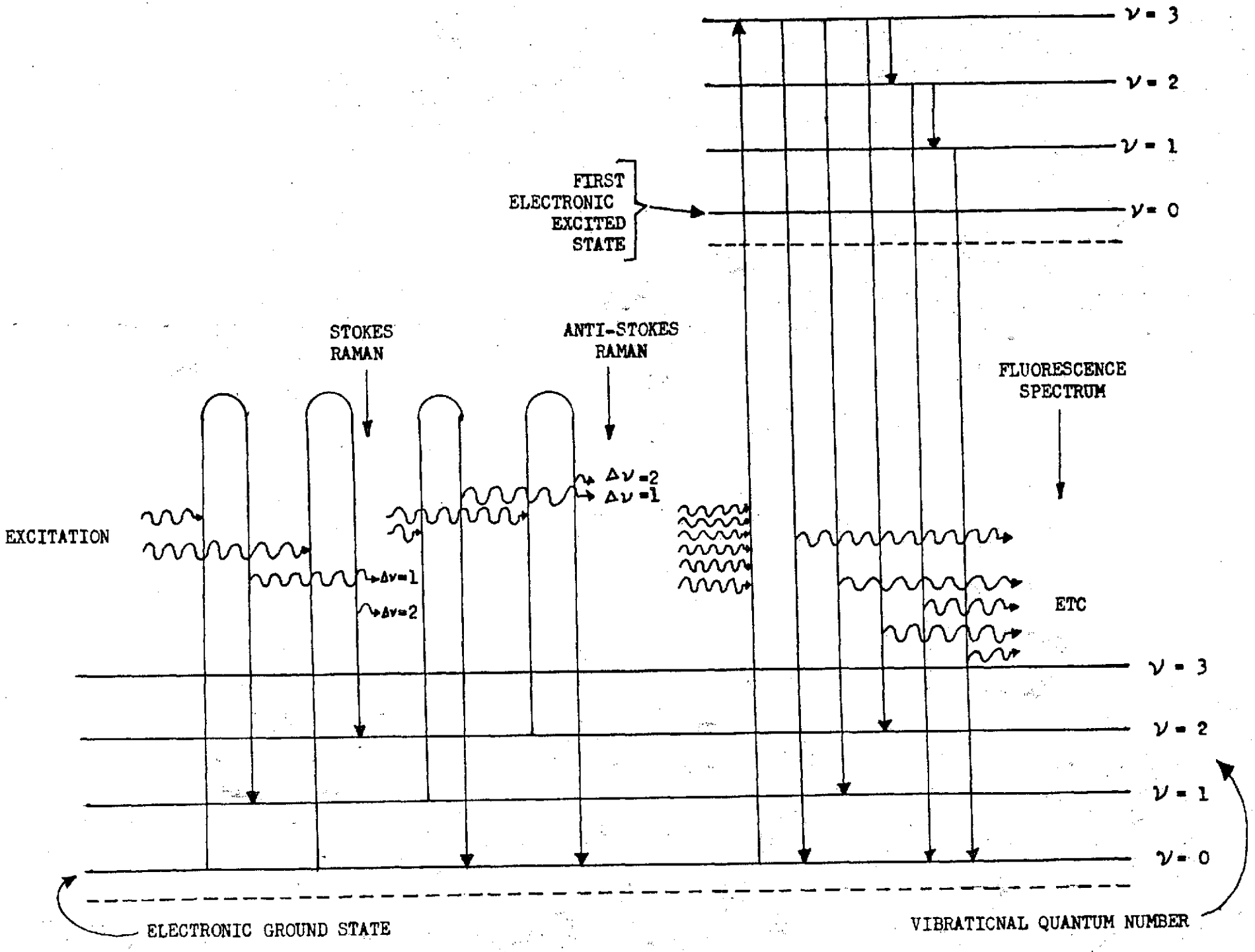

STOKES AND ANTI-STOKES RAMAN AND FLUORESCENCE PROCESSES

FIGURE I

The Raman effect was predicted, sometime before its experimental demonstration by Raman, on the basis of polarization effects of molecules in electromagnetic fields. We do not need to develop any of the theory here, as numerous textbooks on the subject exist.[7,8] Our primary goal here is to outline certain significant results of the theory. The Raman effect is a second order effect (hence its low cross-section) but also this second order dependence allows homonuclear diatomics like nitrogen and oxygen to be observed. As a general rule, since polarizability is a significant parameter, molecules with lots of electrons are good Raman scatterers. Ionic bands, such as occurring in molecules like LiF or HCl will tend to be weaker. Raman scattering is isotropic and the polarization orientation of the incident light relative to the scattered light depends upon the polarization tensor for the particular molecule. Hence one can obtain useful molecular information using this technique.

The overall intensity of Stokes lines for the Raman process is governed by the relation

$$I_s \alpha \frac{(\nu_o - \nu_i)^4}{\nu_i(1 - \exp(-h\nu_i/kT)}$$

and for the anti-Stokes lines

$$I_A \alpha \frac{(\nu_o + \nu_i)^4 \exp(-h\nu_i/kT)}{\nu_i}$$

Hence we have an excellent temperature probe since combining the two equations above gives

$$\frac{I_A}{I_S} = \frac{(\nu_o + \nu_i)^4}{(\nu_o - \nu_i)} \approx e^{-h\nu_i/kT}$$

Experimentally, a spectral scan can be performed over a broad wavelength range on both sides of the excitation wavelength and both Stokes and anti-Stokes bands will be measured. As indicated in the preceding equation and illustrated in Figure 1, the relative intensities of the Stokes and anti-Stokes bands allow the temperature of the sample to be determined. For some strong Raman scatterers, a rotational analysis of the Raman spectrum near the excitation line can be performed and the temperature can be determined independently of vibrational energy levels.

With these concepts in mind, we can now consider what parameters are necessary when evaluating a Raman backscatter experiment. The volume backscatter coefficient for Raman scatter is what we define as the Raman backscatter cross-section per steradian or σ_R.

Hence our working equation for a laser Raman experiment uses what is called the "laser radar" equation. Numerous forms are used, depending on which geometry terms are required.

$$I_S = I_o N L_{\sigma R} G(\lambda, \lambda_R)$$

where

G = Optical geometry parameter

I_o = Total laser photon flux

N = Number density of Raman scatterers

λ_o = Wavelength of incident light

λ_o = Wavelength of Raman emission

σ_R = Raman cross-section

L = Column length detected

Several calculations have been performed using this equation. Our goal was to vary certain parameters such as azimuth angle and height (i.e., distance from source) and power. Compromises in power and distance resolution had to be maintained since a more powerful pulse will in general have a longer pulse duration. An optimization study with the Raman backscatter equation allows one to determine detectability levels for a particular Raman cross-section. Results of this approach are included in Section D.

C. INSTRUMENTATION

The present trends in laser Raman spectroscopy for remote sensing parallels the trends in laboratory based instrumentation. Thus a high power laser is used for excitation while photon-counting appears to be the most preferred approach for signal analysis. This is quite understandable since Raman cross-sections are very small ($\sim 10^{-30}$ cm^2) and the Raman signals can be extremely weak. However, in setting up a remote sensing experiment one usually desires also to measure the distance at which the Raman emitters reside relative to the receiver. For this reason, remote sensing prefers a pulsed laser, which has the added advantage that it also initiates all timing sequences for distance measurements. The greater specific power of a pulsed laser also enhances the absolute photon flux for the Raman process itself. Gated photon counting techniques then allows one to measure the Raman intensities from specific distances to be measured individually. Ideally one can obtain a maximum amount of geographical information by using multichannel analyzer or minicomputer techniques to store the Raman emissions over the time scale. The references presented within this report illustrate the variety of techniques used for remote sensing, but most of them do adhere to the concepts above. A typical arrangement as given by Schildkraut[6] is given in Figure II.

Note that in this arrangement a large Cassegrainian telescope is used to collect a maximum amount of the return signal. The collecting optics are usually a 16-36 inch mirror. There are a

FIGURE II REMOTE RAMAN SPECTROMETER LAYOUT

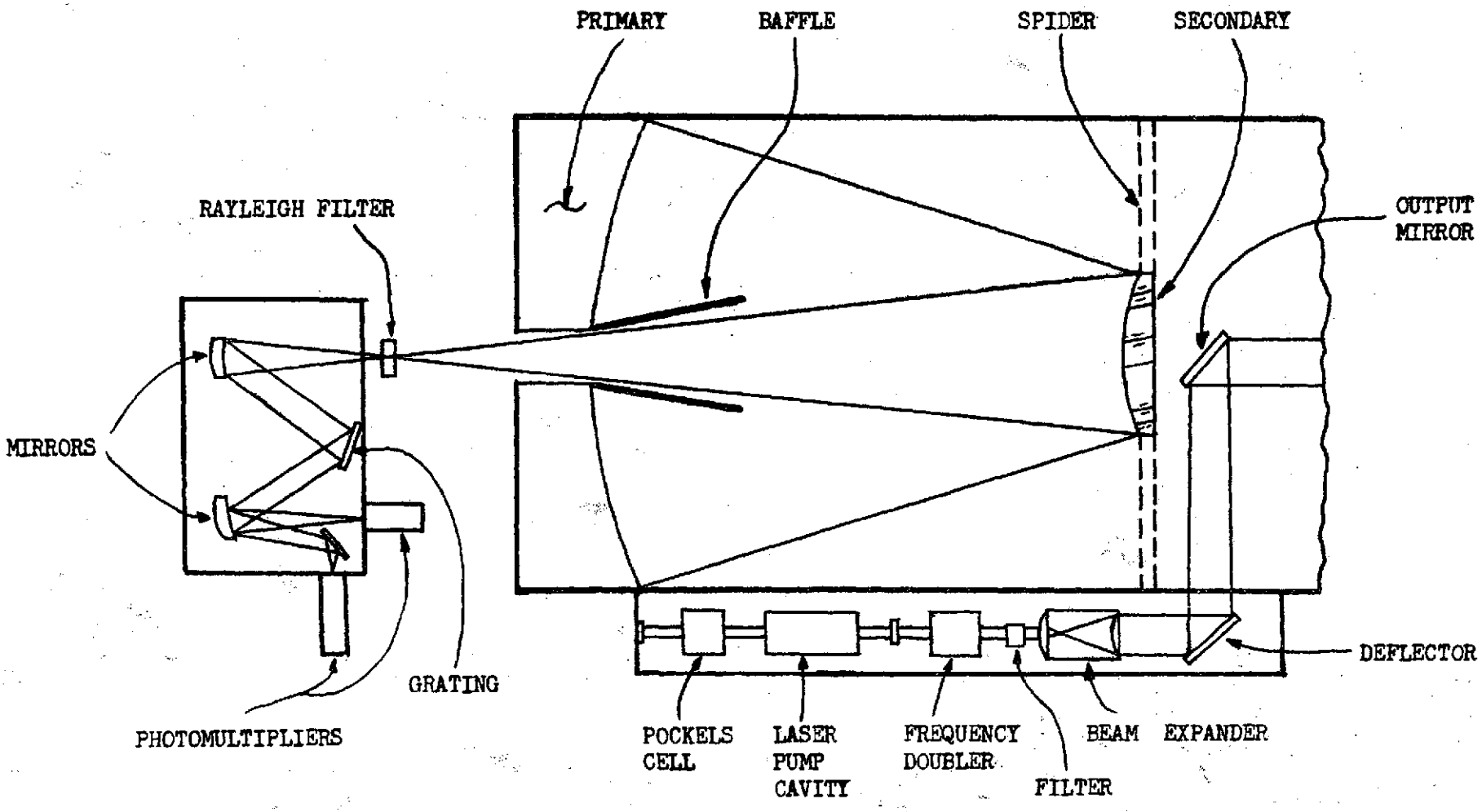

FIGURE III

EXCITATION LINE = 632.8 nm

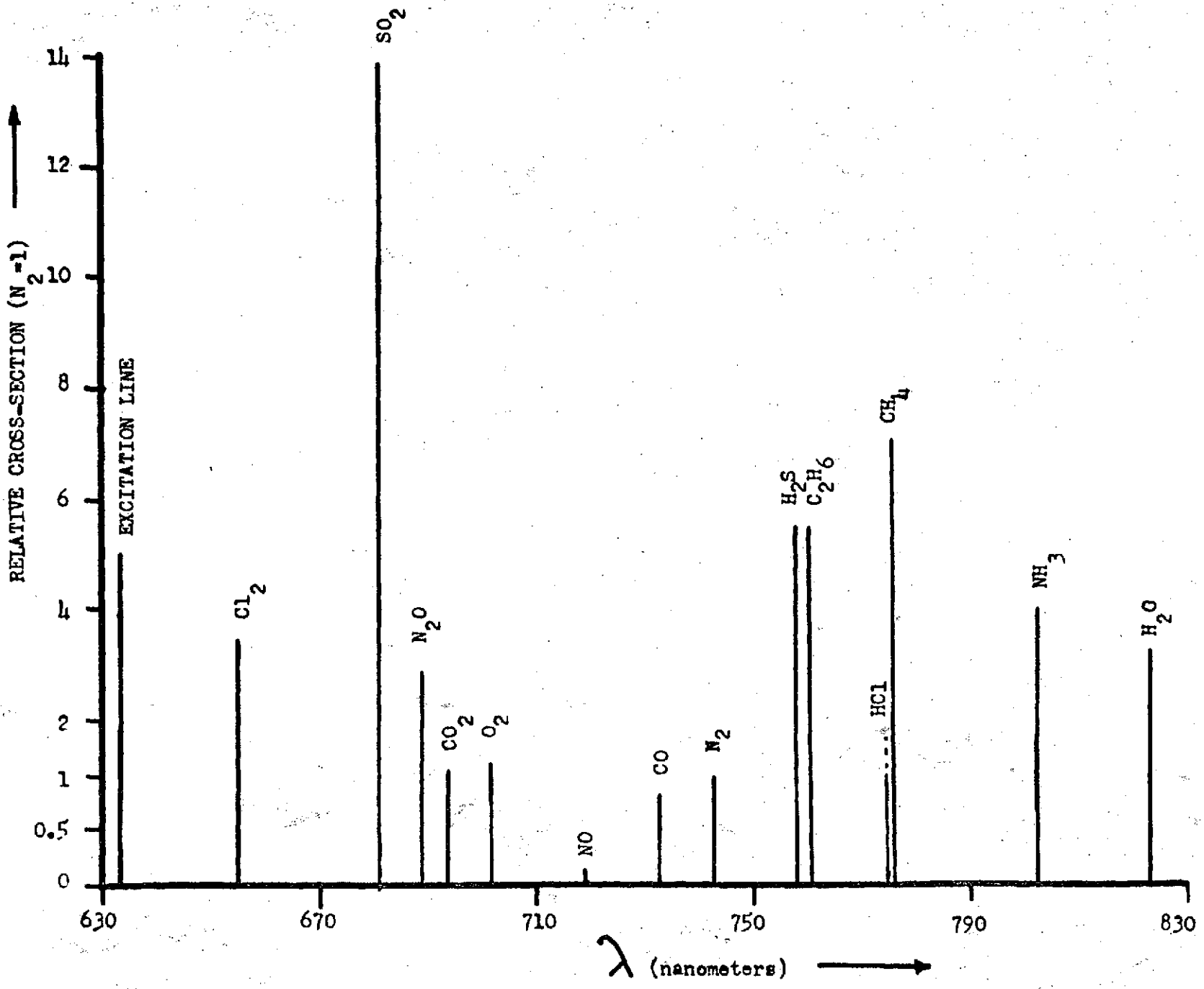

FIGURE IV **EXCITATION LINE = 488.0 nm**

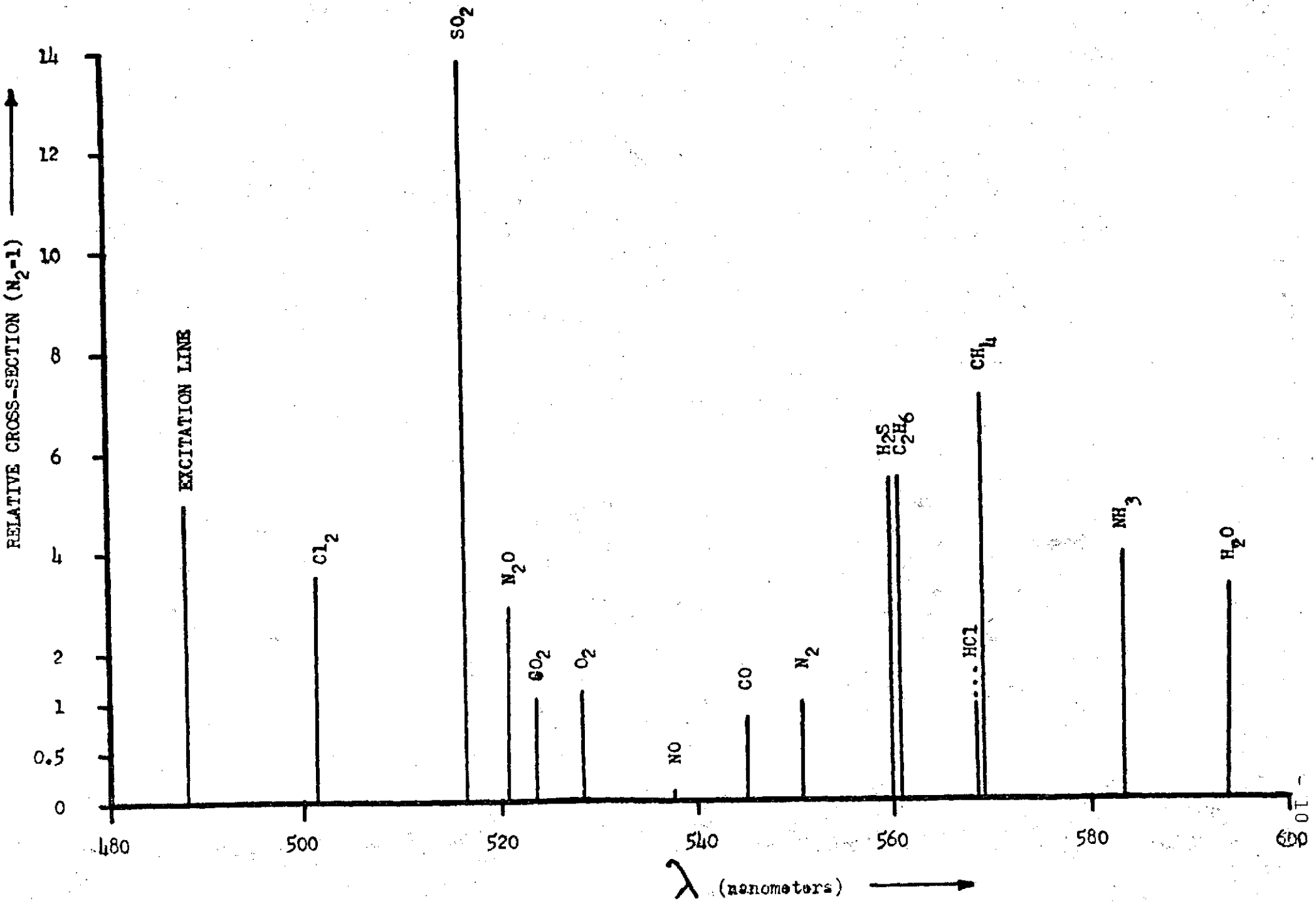

FIGURE V EXCITATION LINE = 347.2 nm

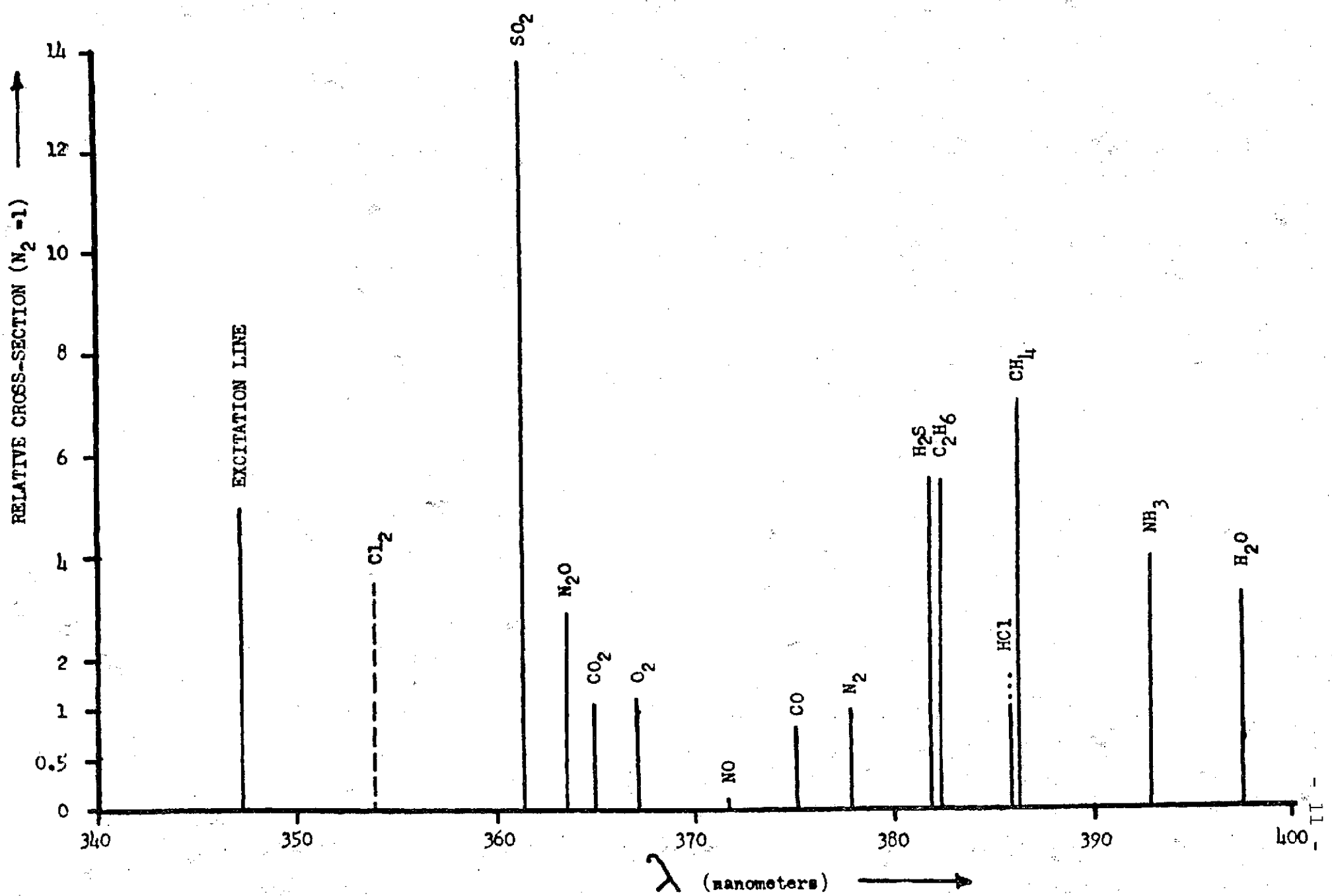

FIGURE VI EXCITATION LINE = 337.1 nm

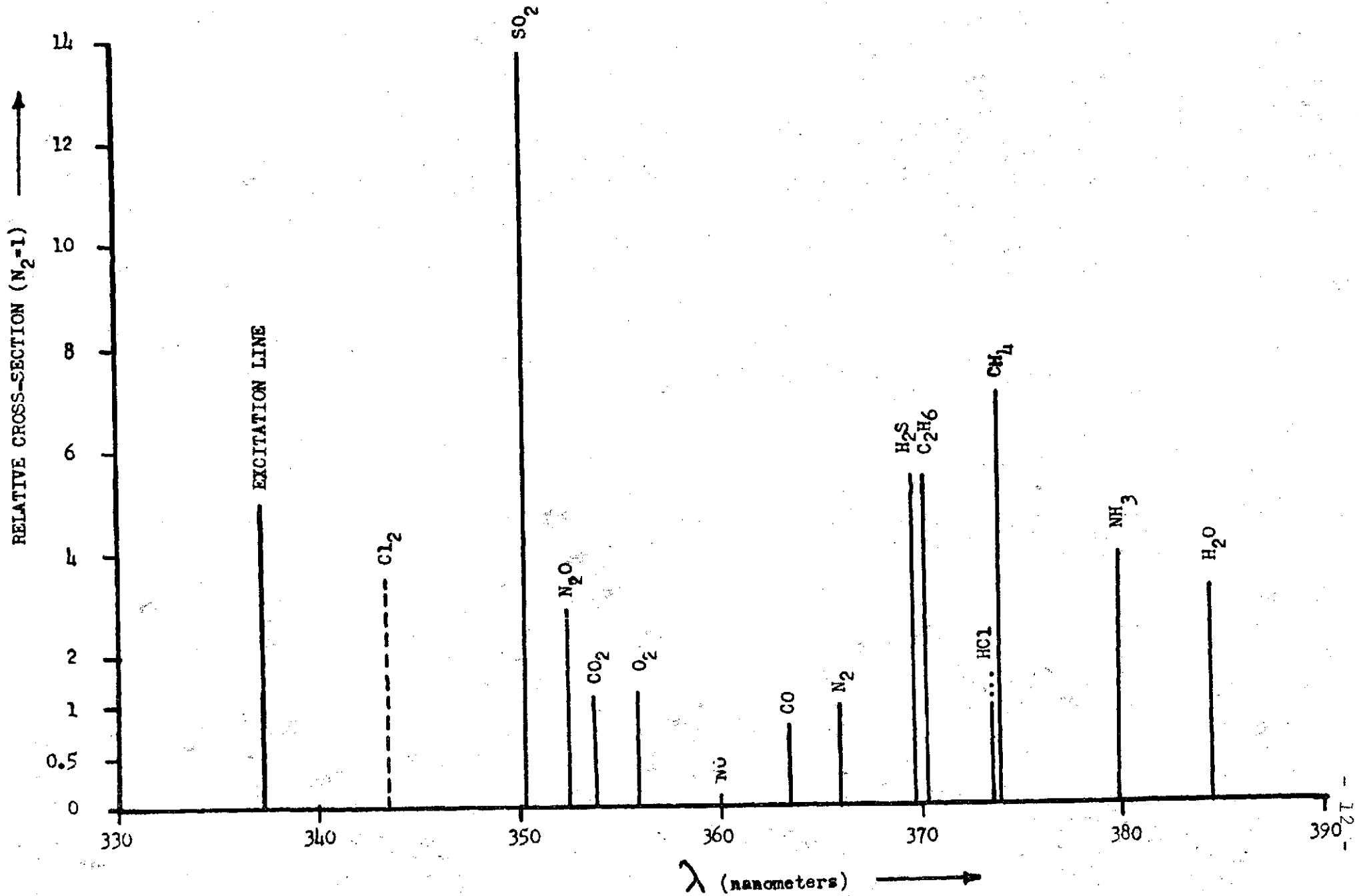

FIGURE VII EXCITATION LINE = 265.0 nm

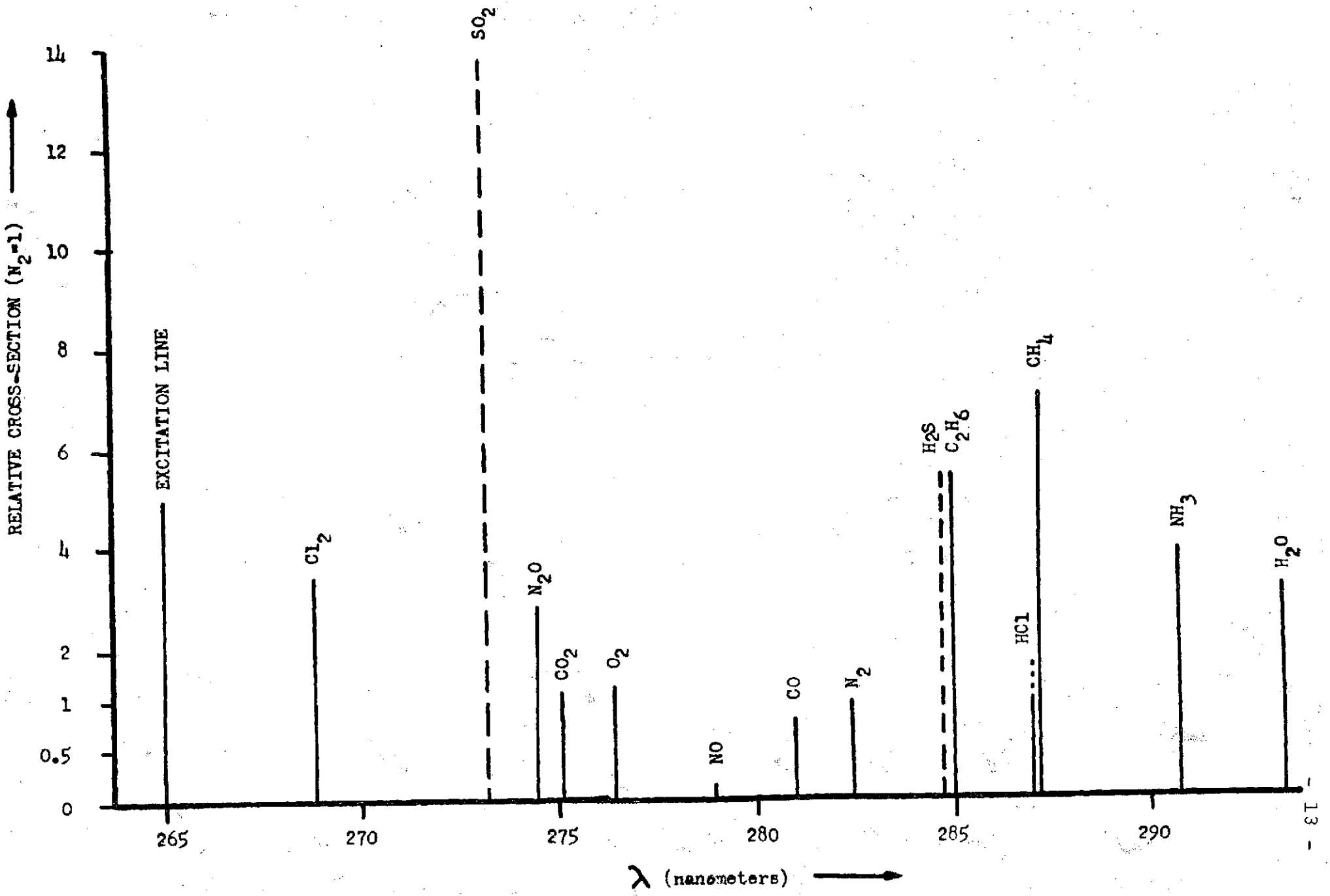

number of telescopic systems which can work, but the Cassegrainian system offers several advantages: (1) spherical aberrations can be made zero; (2) all other aberrations are negligible for small fields-of-view; (3) it is convenient geometry for coincident line-of-sight between the laser and the collector; (4) the physical length of the telescope system is only 25% of the effective optical focal length (providing a relatively compact unit); and (5) stray light baffling of a Cassegrian telescope is straight forward. One cannot overemphasize the necessity for eliminating stray light in order to improve upon the overall sensitivity.

The type of spectral analyzer used for a remote sensing system varies according to whether the experiments need to be broadband in order to observe many different molecular emissions or are intended for just a few specific molecules. In the latter case spectral filters with 2.0-5.0 nm bandwidth are usually sufficient. Each molecular Raman signal is unique for a particular laser source. Figures III to VII identify the spectral band positions for the more popular types of lasers which would be useful for laser Raman studies. Hence for the monitoring of specific molecules with a particular laser, spectral characteristics like these will enable one to determine which spectral filters produce the desired result.

However, for the broadband applications, which is most convenient for a large number of spectral bands and for a greater degree of specificity (i.e., higher resolution), a monochromator is the more appropriate spectral analyzer. In terms of stray light elimination, a monochromator is much more efficient than spectral filters and

for laboratory studies, double and even triple monochromators are used primarily for their efficiency in producing stray light (from the exciting wavelength) ratios of 10^{-11} and better. In terms of sensitivity, a monochromator detector will actually "see" a smaller fraction of the desired signal; however (especially with photon counting), a lower noise level is obtained. Because of the reduction in intensity of the signal with higher order monochromators, remote sensing systems usually use single or double monochromators and gated photon counting for distance resolution.

Extensive research in the development of sensitive Raman instrumentation and in expanding the available commercial instrumentation useful for remote Raman experiments have made this technique very useful for molecular measurements. In spite of the relatively insensitivity of the Raman effect as compared to absorption, these instrumental developments have made the technique highly acceptable for remote measurements.

D. RAMAN CROSS-SECTIONS OF MOLECULAR SPECIES

Probably the most significant data obtained in the laboratory, which can be utilized in remote sensing, is knowledge of Raman cross-sections of molecular species. Since the technological developments in laser Raman instrumentation have been evolving rapidly into more sophisticated systems, most emphasis has been placed in this area. Now that good instrumentation is available, more research should be placed in the area of molecular cross-sections. A listing of some known cross-sections for molecules of interest is given in Table 2.

Figure VII illustrates some results from our calculations on detection limits for a typical laser Raman experiment. The known cross-sections for water, nitrogen, and oxygen are used for this calculation. Obviously the further away the target molecules, the less intense the Raman signals. It is interesting that at distances less than 100 meters, molecular concentrations of 10^{13}-10^{14} can be detected for $\sigma_R \sim 10^{-29}$ or less. Hence if any enhancement (resonance Raman) occurs, much lower concentrations will be detectable.

TABLE 2

RAMAN CROSS SECTIONS

Compound	Raman line shift $\Delta\nu$, cm^{-1}	Relative cross section compared to nitrogen	Cross section at 4880 A and 180° observation angle $cm^2\ molec^{-1}$
Ammonia	3340	3.98	2.80×10^{-20}
Carbon dioxide	1388	1.18	8.30×10^{-20}
Carbon monoxide	2143	0.81	5.69×10^{-30}
Chlorine	540	3.46	2.43×10^{-29}
Ethane	2650	5.50	3.87×10^{-29}
Hydrogen	530	6.29	4.42×10^{-29}
Hydrogen sulfide	2611	5.55	3.90×10^{-29}
Methane	2914	7.15	5.02×10^{-29}
Nitric oxide	1887	0.08	5.62×10^{-31}
Nitrogen	2331	1.00	7.03×10^{-30}
Nitrous oxide	1290	2.90	2.04×10^{-29}
Oxygen	1555	1.21	8.51×10^{-30}
Sulfur dioxide	1120	13.80	9.70×10^{-20}
Water (vapor)	3652	3.24	2.28×10^{-20}
Hydrogen chloride	2990	Unknown	Unknown

FIGURE VII MOLECULAR CONCENTRATION VS. RANGE

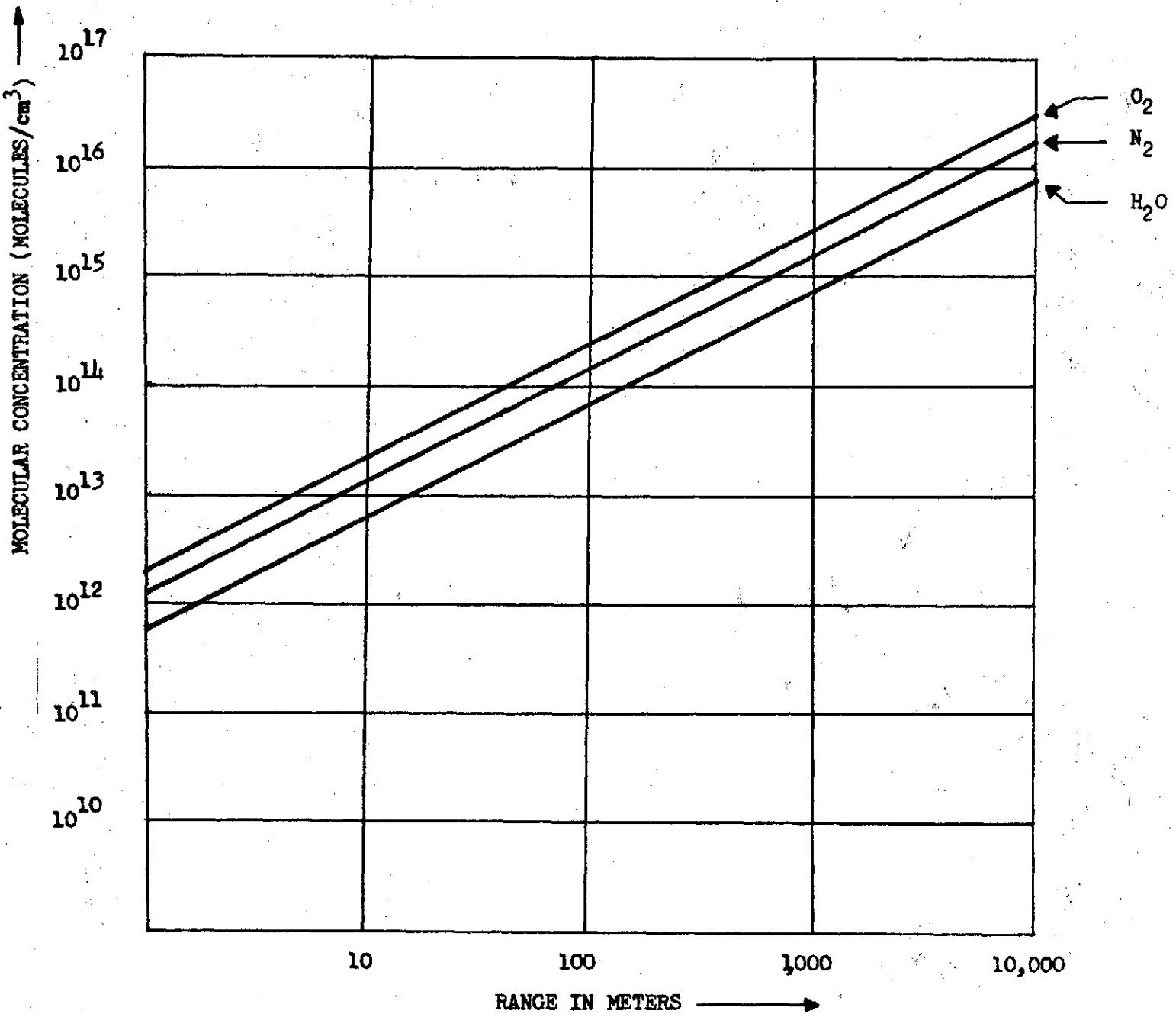

1. TRANSMITTER:

   Wavelength - 488.0 nm
   Peak Power - 1 Joule

2. RECEIVER:

   Optical Efficiency - 20%

3. MOLECULAR PARAMETERS USED:

Molecule	Raman Cross-Section	Raman Wavelength
H_2O	2.28×10^{-29}	3652 Å
N_2	7.03×10^{-30}	2331 Å
O_2	8.51×10^{-30}	1555 Å

E. EXPERIMENTAL RESULTS

In order to provide a remote sensing program with sufficient information for analyzing the data obtained, it is necessary that some laboratory experimentation be performed in order to provide accurate information on molecular cross-sections and wavelengths. The experiments carried out here used a Cary 81 Raman Spectrophotometer and a Spectra physics 164 Argon Ion Laser. Sample containers included a stainless steel chamber (single pass, 180^0 incidence), a multi-pass cell (20 passes maximum), and the atmosphere itself. Ordinarily a quartz lens focussed the laser beam into a very narrow line and the light emitted from this volume was collected by the fore optics of the Cary 81. Although this particular instrument was intended for Toronto Arc excitation, these laser excitations performed satisfactorily. Unfortunately, we were unable to utilize photon counting in these experiments since the Cary 81 electronics package and photomultiplier tubes were not appropriate to innovate photon counting into the signal processing.

Examples of the spectra obtained in this manner are shown in Figures VIII - XI. Our results compared favorably with the ones presented in references 1-5. Since our approach was primarily feasibility, we did not try to obtain any absolute cross-sections.

It is significant to note that we obtained unusual results with HCl in the multi-pass cell. The Raman peak should occur at 2990 cm^{-1} away from the excitation line. Our results are illustrated in Figure XI. Notice that we obtained two peaks at 3068 and at 3216

cm^{-1}. We have not been able to explain this result at the present time. It is a problem which justifies further research, especially since HCl is becoming more of a problem in aeronomic considerations.

FIGURE VIII ATMOSPHERIC N_2 IN MULTIPASS GAS CELL

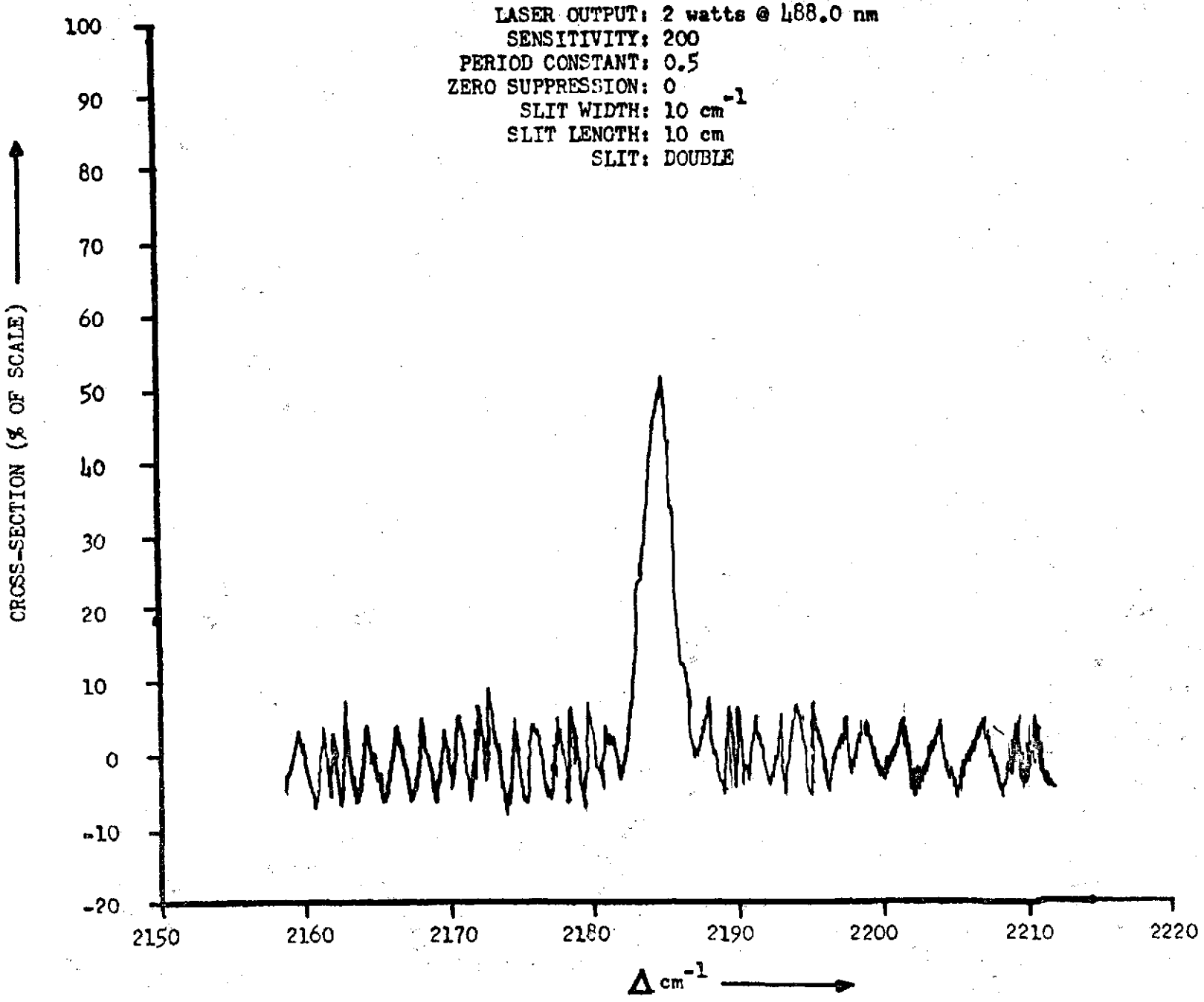

FIGURE IX 90% O_2 IN MULTIPASS GAS CELL

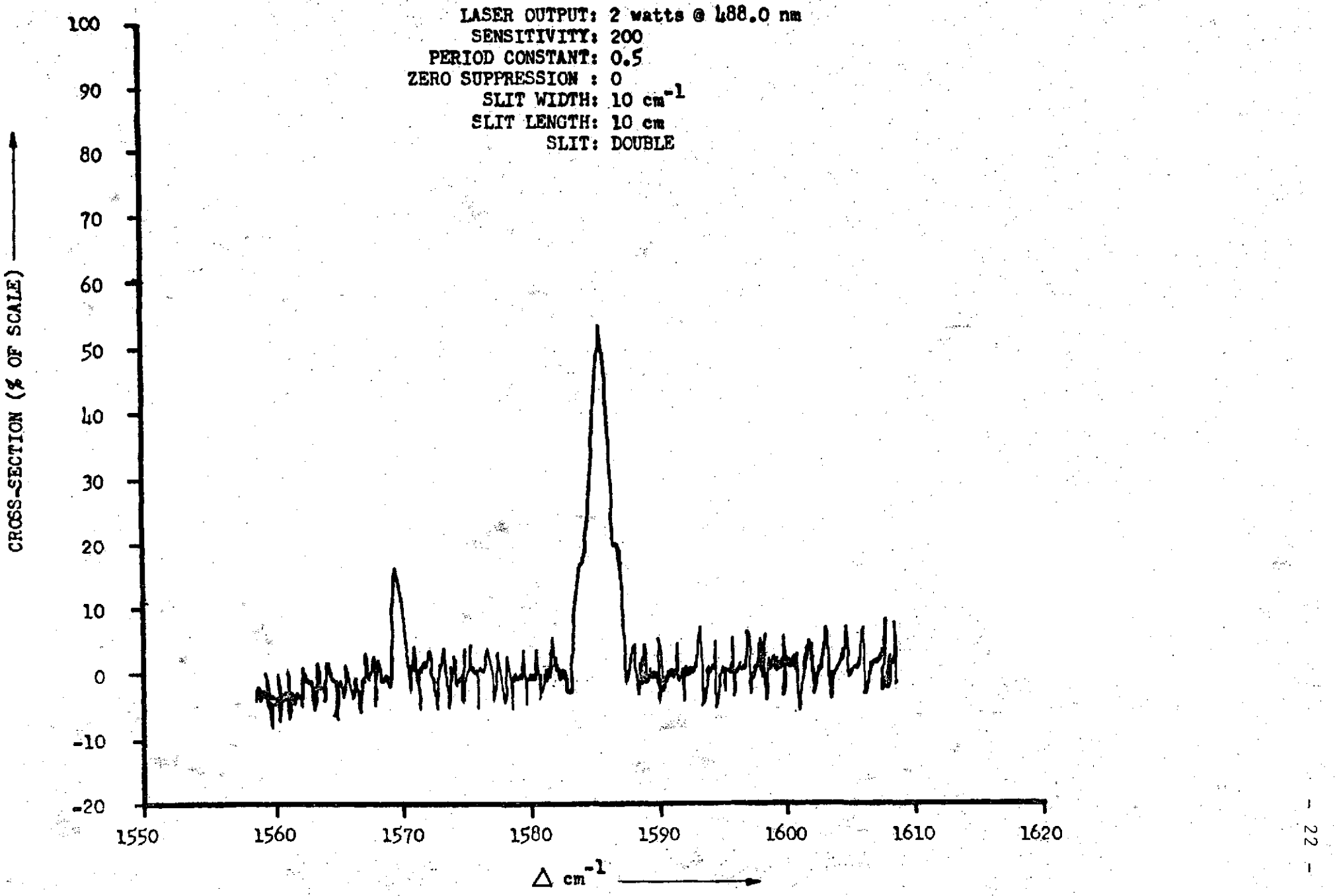

FIGURE X 90% SO_2 IN SINGLE PASS GAS CELL

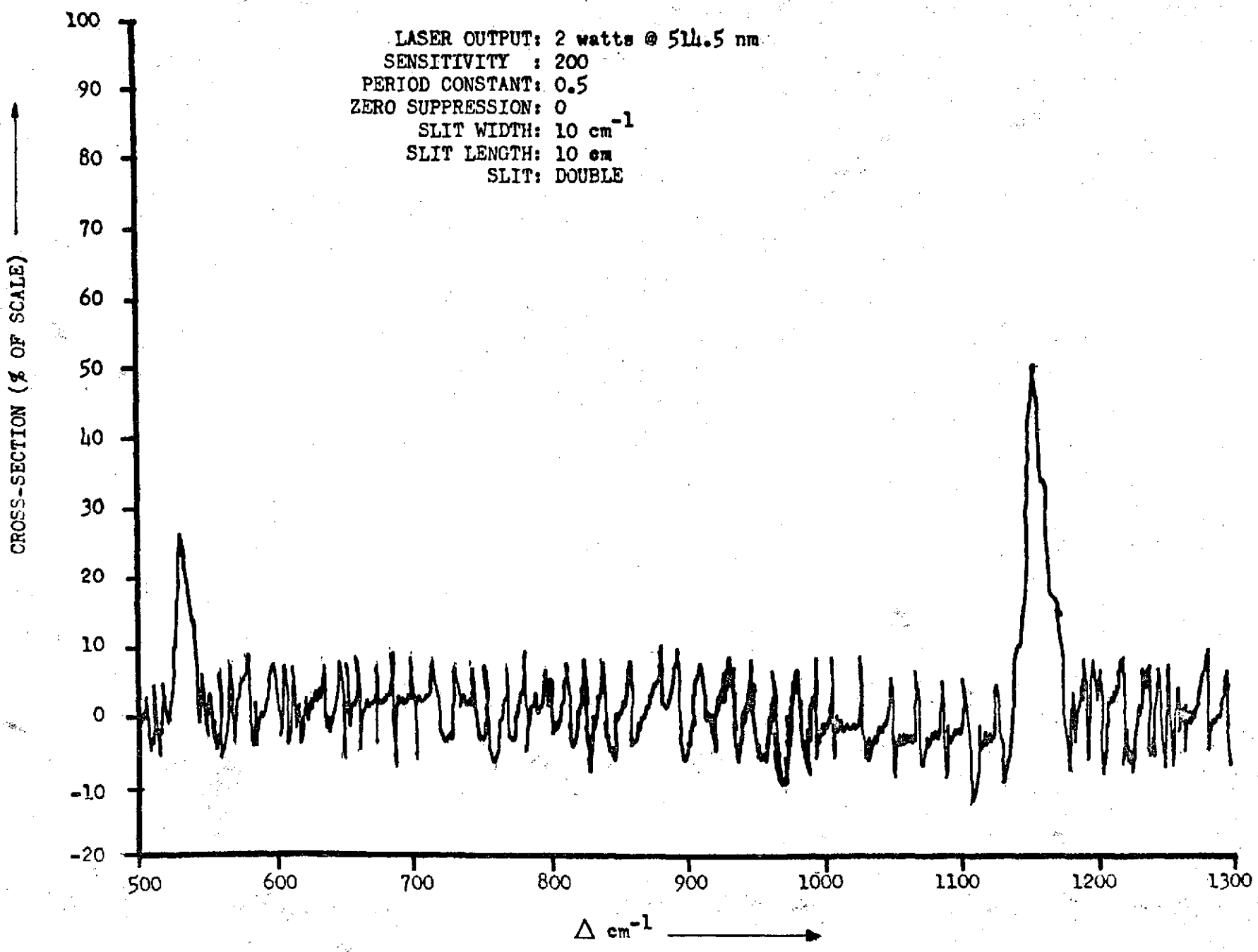

FIGURE XI 90% HCl IN MULTIPASS GAS CELL

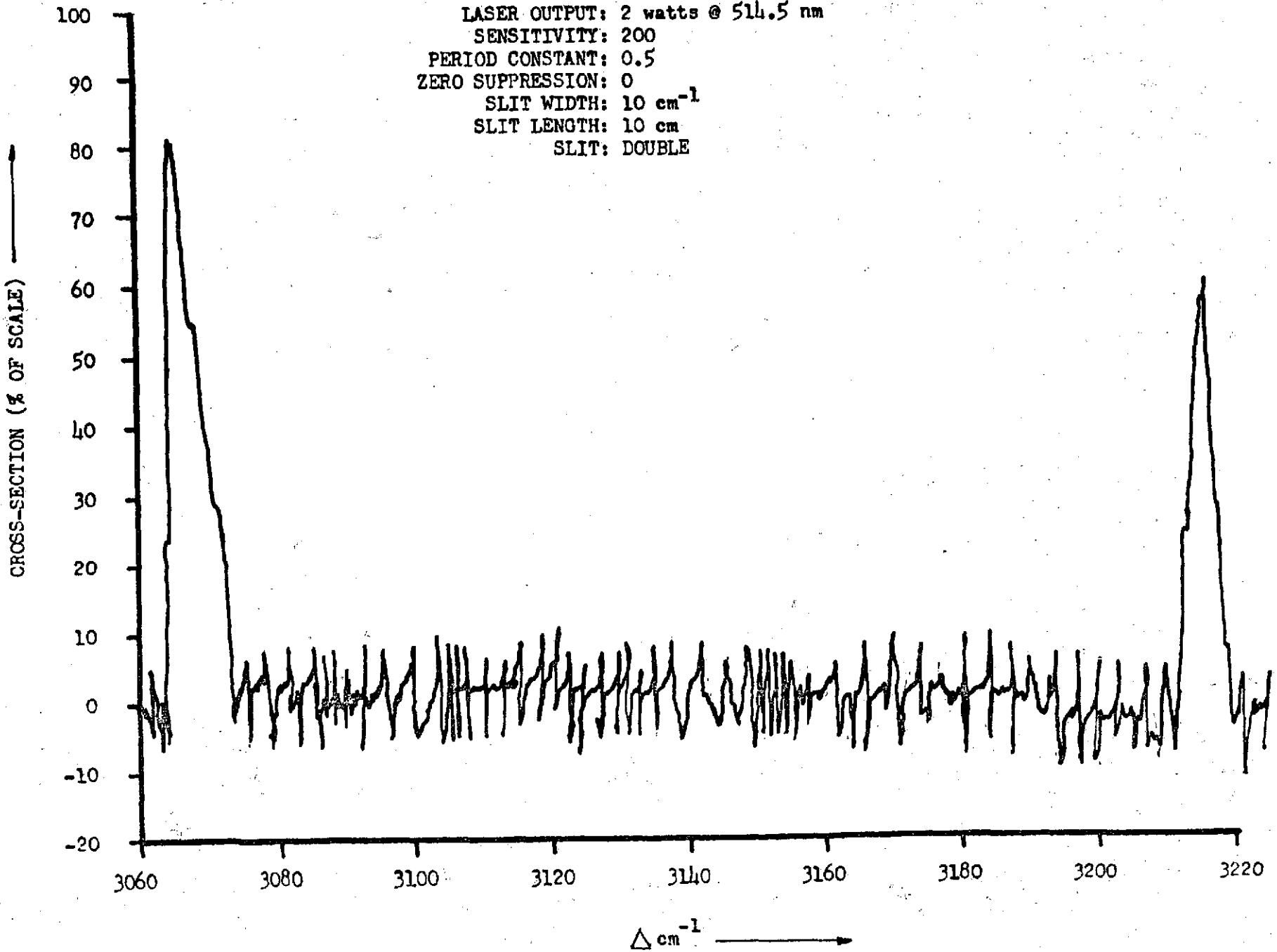

F. APPLICATIONS TO ATMOSPHERIC PROCESSES

In considering what experimental hardware is desirable for applying Raman backscatter experiments, we need to first consider the lasers which are available. Table 3 lists the principle types of lasers which have been used or considered for atmospheric studies. For Raman backscatter measurements, visible wavelength lasers are more popular; but more attention is being paid to uv emitters such as the N_2 laser, doubled ruby or quadrupled Nd-yag. It is anticipated that the increased Raman cross-section at the shorter wavelengths will provide a greater return signal than the excitation signal loses to the atmosphere.

A survey of experiments already carried out is given in Table 4. Included in this table is a listing of the observable measured. Thus one sees that there are numerous parameters which are measurable by remote laser probes. The use of laser Raman exclusively will enable such parameters as molecular concentrations, mixing ratios, and temperature profiles to be measured.

As an example, consider the estimated molecular concentrations for the atmospheric species in Figure XII. Applying the results given in Figure VII, it is obvious that for simple Raman cross-section, the Raman signal can be weak indeed. However, if enhanced Raman or fluorescent signals are possible, then species such as OH will be measurable at distances less than 100 km.

TABLE 3

OUTPUT POWER OF FIXED FREQUENCY AND TUNABLE LASERS

Type of Laser	Wavelength (nm)	Single-Mode c.w. Output (w)	Pulsed Output Peak Power or Energy	Pulse Rate (pp)
Ruby	694.3	-	125 J	Single-shot
Ruby SHG	347.2	-	5 J	
ND-Yag	1064.0	25(1000)	650 J	Single-shot
Nd-Yag SHG	532.0		26 J	
N_2-laser	337.1		10^7 w	500
Noble gas ion				
Ar	488.0/515.0	40(150)	2000 w	10^6
Ar	351.1/366.8	5	250 w	10^6
KR	647.1	4	200 w	10^6
Chemical laser				
HF	2600-3600	4500	10 J	Single-shot
HCl	3500-4100	560	1 J	Single-shot
DF	3600-5000	4500	10 J	Single-shot
High-pressure gas laser				
CO	4800-8500		300 J	Single-shot
CO_2	9100-13000	10^4	500 J	Single-shot
Organic dye	340-1200	5×10^{-2}	10^7 w	100
Parametric oscillator	500-4000	3×10^{-3}	10^5 w	10^3
Spin-flip Raman	5300-14000	1	10^3 w	10^3
Semiconductor diode	320-34000	5×10^{-2} (0.25)	10^2 w	

TABLE 4. SURVEY ON LASER PROBING OF THE ATMOSPHERE

Investigator	Technique Used	Laser	Wavelength (nm)	Peak Power and Energy (w)/(J)	Telescope Diameter (cm)	Filtering Devise	Measurement	Refs.
Melfi, Lawrence, Jr.	Elastic scattering	Ruby & SHG	694.3 347.2	10^8	40	-	Aerosol	9
McCormick	Raman scattering	Ruby SHG	347.2	$2x10^6$/0.04J	40	Double-Monochr	N_2,O_2,H_2O profiles	10
Kent, Wright, Sandland	Elastic scattering	Ruby	694.3	$2x10^6$/7J	$16m^2$	Infrared filter 2nm	Atmospheric density & tide	2
Sandford, Bowman, Gibson	Elastic scattering	Ruby	694.3	$2x10^6$/5J	30	-	Atmospheric density & aerosol	11
	Resonance	Tunable	589.6	$5x10^4$/0.01J	$0.6m^2$	-	Atmospheric sodium layer	12
Reagan, Herman	Mie scattering	Ruby	694.3	10^8/0.8J	20	Infrared filter 1.4nm	Aerosols	13
Boneditti-Michelangeli et al.	Mie scattering	Argon-ion	488.0	0.2(c.w.)	50	Fabry-Perot	Aerosol motion, wind velocity	14
Cooney	Raman scattering	Ruby	694.3	$2.5x10^8$/2.5J	75	Infrared filter 1.5nm	N_2	15

TABLE 4 CONTINUED

Investigator	Technique Used	Laser	Wavelength (nm)	Peak Power and Energy (w)/(J)	Telescope Diameter (cm)	Filtering Devise	Measurement	Refs.
Cooney (cont)		Ruby & SHG	347.2	1.8×10^7	75	Infrared filter 1nm	H_2O, N_2 profiles	16
		Ruby	694.3	8×10^7/20J	$1m^2$	Infrared filter 0.7nm	Temperature profile	17
Strauch, Derr, Cupp	Raman scattering	N_2 laser	337.7	$10^3/10^{-3}$J	35	Infrared filter	N_2 (temp. profile) H_2 profile	18
Leonard	Raman scattering	N_2 laser	337.1	$10^5/10^{-3}$J	20	Infrared filter 3.5nm	N_2, O_2	19
		N_2 laser	337.1	2.5×10^4	25	Monochro-mator	N_2, O_2, CO_2, H_2O	20
Inaba, Kobayasi, Nakahara	Raman scattering	Ruby	694.3	10^7/0.15J	30	Monochro-mator	N_2, O_2, SO_2, CO_2	21
		N_2 laser	337.1	$2 \times 10^4/10^{-4}$J	30	Monochro-mator	Air pollutant	22
		Nd-Yag	532.0	$7 \times 10^5/7 \times 10^{-3}$J	50	Infrared filter 0.4nm	SO_2	

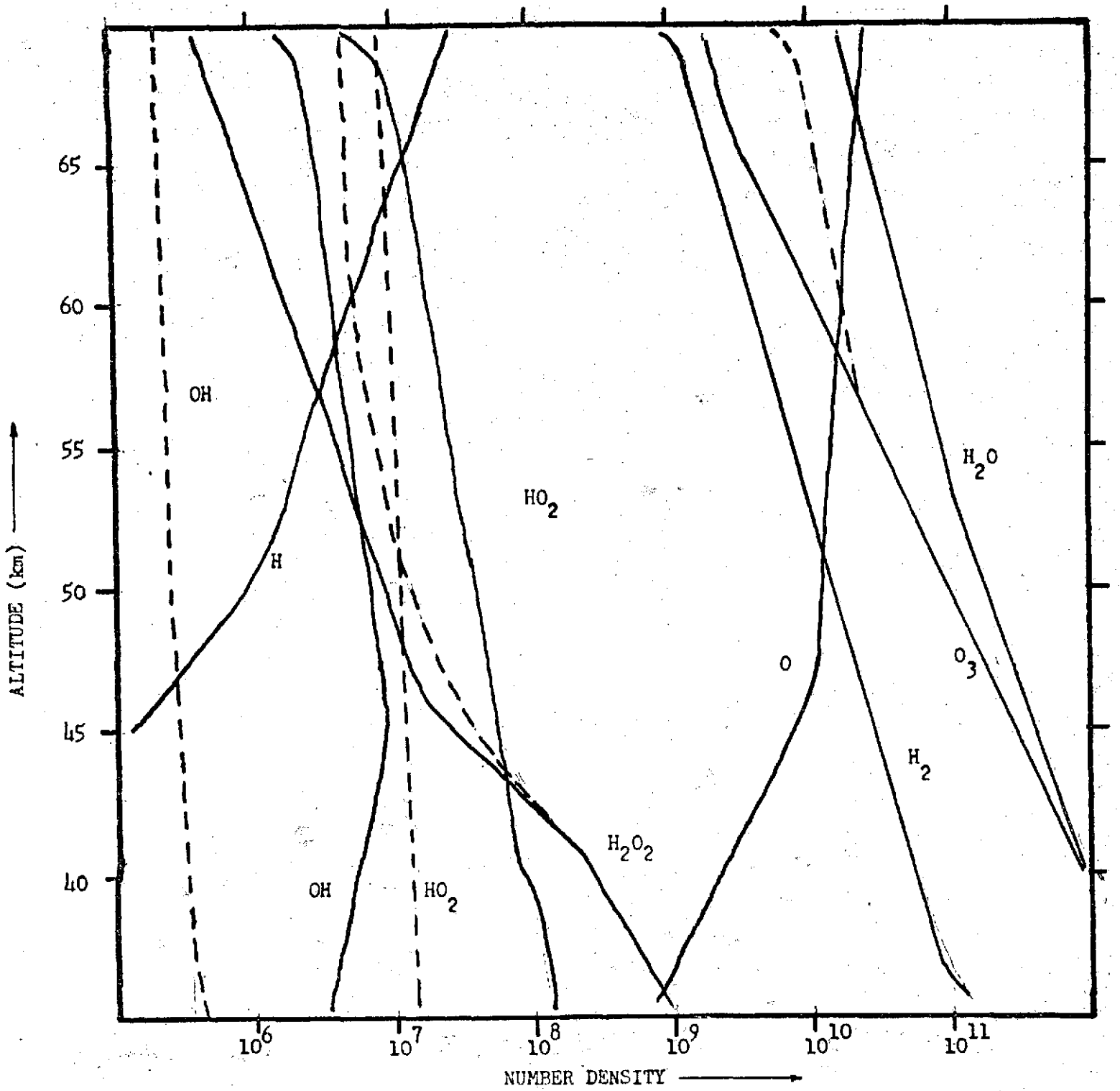

Figure XII Noon values given by solid curves;in case of diurnal variation midnight values are broken

G. RECOMMENDATIONS FOR FURTHER LABORATORY RESEARCH

In order that this feasibility study develop into a worth while program, it is necessary to formulate a laboratory study which can evolve into flight experimentation. The present laser systems available are sufficient for this purpose. The argon ion or argon-krypton ion laser is certainly the most versatile for laboratory studies. Two other laser systems deserve consideration for their ultraviolet excitation lines. The nitrogen laser and the doubled ruby laser have both been used successfully, both in the laboratory and in the field. It is advantageous at this time to also consider the quadrupled Nd-YAG laser since all the Raman emissions shown in Figure VII occur below 300 nm. This means that daylight experiments can be performed below the ozone layer of the atmosphere using a solar blind photomultiplier tube to reduce background photons. Balloon flights would be an obvious approach for solar blind experiments.

The laboratory experiments most needed at this time appear to be Raman cross-section measurements at various wavelengths. Initially the results of excitation at 488.0 and 514.5 nm for molecular species like ozone, hydrogen chloride, nitrogen oxides and organic trace species in the aromatic and aldehyde groups would be useful. Extension of these cross-sectional data to shorter wavelengths is necessary if due consideration can be made to choosing flight laser systems. For instance, at this time there is nothing in the literature about measurements from 265 nm excitation. In order to predict the use-

fulness of a specific laser, more detailed information on Raman cross-sections has to become available.

Another area of importance is investigating the utility of the tuned laser to atmospheric sensing so that molecular species such as OH, Na, and others can be monitored remotely. Tunability will enable the experimentalist to achieve a maximum return signal by using the wavelength which provides an enhanced process, such as the resonance Raman process.

At the present time it is worthwhile to begin a laboratory program emphasizing Raman backscatter cross-sections of significant molecular species, and the extension of the Raman pump frequency further into the ultraviolet. The data obtained from this program will enhance the development of experiments to benefit flight programs and provide direction for such programs, as well as provide significant data for these programs.

BIBLIOGRAPHY

1. Northend, C. A., Honey, R. C., and Evans, W. E., "Rev. of Scientific Instruments," 37, 393 (1966).

2. Kent, G. S. and Wright, R. W. H., "Jour. of Atmos. and Terr. Physics," 32, 917 (1970).

3. Derr, V. E. and Little, C. G., "Applied Optics," 9, 1976 (1970).

4. Derr, V. E., "Remote Sensing of the Troposphere," published by U. S. Government Printing Office.

5. Wang, C. P., "Impact of Aerospace Technology on Studies of the Earth's Atmosphere," pages 105-123, Pergamon Press, 1974.

6. Schildkraut, R., "Laboratory Instrumentation Spectroscopy," Series I, Volume II, p.303-312, published by International Scientific Communications, Inc., Green Farms, Conn., 1974.

7. Tabin, Marvin C., "Laser Raman Spectroscopy," Wiley-Interscience New York, 1971.

8. Gilson, T. R. and Hendra, P. J., "Laser Raman Spectroscopy," Wiley-Interscience, New York, 1970.

9. McCormick, M. P., "Electro-Optics International Conference," Bringhton, England (March 24-26, 1971).

10. Melfi, S. H., "Applied Optics," 11, 1605-1610 (1972).

    Melfi, S. H., Lawrence, Jr., J. D. and McCormick, M.P., "Appl. Phys. Lett.," 15, 295-297 (1969).

11. Sandford, M. C. W., "Atmos. Terr. Phys.," 29, 1657-1662 (1967).

12. Sandford, M. C. W. and Gibson, A. J., "J. Atmso. Terr. Phys.," 32, 1423-1430 (1970).

13. Reagan, John A. and Herman, B. M., "14th Radar Meteorology Conference," Tucson, Ariz. (November 17-20, 1970).

14. Beneditti-Michelangeli, G., Congeduti, F. and Fiocco, G., "J. Atmos. Sci.," 906-910 (1972).

15. Cooney, J. A., "Appl. Phys. Lett.," 12, 40-42 (1968).

16. Cooney, J. A., "J. Appl. Meteorology," 9, 182-184 (1970).

17. Cooney, J., "J. Appl. Meteorology," 11, 108-112 (1972).

18. Strauch, R. G., Derr, V. E. and Cupp, R. E., "Applied Optics," 10, 2665-2669 (1971).

19. Leonard, D. A., "Nature," 213, 142-143 (1967).

20. Leonard, D. A., AVCO Everett Res. Lab. RR-362 (December 1970).

21. Inaba, H. and Kabayasi, T., "Appl. Phys. Lett.," 17, 139-141 (1970).

22. Inaba, H. and Kobayasi, T., "Optic-electronics," 4, 101-123 (1972).